New Materials Approaches

Mater. Res. Soc. Symp. Proc. Vol. 1543 © 2013 Materials Research Society
DOI: 10.1557/opl.2013.954

A new thermoelectric concept using large area PN junctions

R. Chavez, A. Becker, V. Kessler, M. Engenhorst, N. Petermann, H. Wiggers, G. Schierning, R. Schmechel
Faculty of Engineering and Center for NanoIntegration Duisburg-Essen (CENIDE), University of Duisburg-Essen, 47057 Duisburg, Germany

ABSTRACT

A new thermoelectric concept using large area silicon PN junctions is experimentally demonstrated. In contrast to conventional thermoelectric generators where the n-type and p-type semiconductors are connected electrically in series and thermally in parallel, we demonstrate a large area PN junction made from densified silicon nanoparticles that combines thermally induced charge generation and separation in a space charge region with the conventional Seebeck effect by applying a temperature gradient parallel to the PN junction. In the proposed concept, the electrical contacts are made at the cold side eliminating the need for contacts at the hot side allowing temperature gradients greater than 100K to be applied. The investigated PN junction devices are produced by stacking n-type and p-type nanopowder prior to a densification process. The nanoparticulate nature of the densified PN junction lowers thermal conductivity and increases the intraband traps density which we propose is beneficial for transport across the PN junction thus enhancing the thermoelectric properties. A fundamental working principle of the proposed concept is suggested, along with characterization of power output and output voltages per temperature difference that are close to those one would expect from a conventional thermoelectric generator.

INTRODUCTION

In recent years non-fossil fuels and efficiency of energy conversion have gained great interest as the world prepares to fulfill the projected energy demand. In regards to the later, thermoelectricity could play an important role by allowing a practical form of heat waste recovery as nearly 60% of the energy consumed in the U.S.A. is wasted in the form of heat[1]. Although efforts are being done to incorporate thermoelectric generators (TEGs) in automobiles, among other difficulties, the relatively low efficiencies, usually between 5-15% [1], have refrained the application of thermoelectric generators to deep space missions [2,3]. However, the reduction of the thermal conductivity in nanostructured materials has brought improvements to the thermoelectric material's figure of merit [4–6] and thus the efficiency of the energy conversion process defined by the operation temperatures and the figure of merit which is usually written as:

$$zT = \frac{\sigma \alpha^2 T}{\kappa} \quad (1)$$

where T is the temperature, σ is the electrical conductivity, α the Seebeck coefficient and κ the thermal conductivity.

Conventional thermoelectric generators consist of p and n-type semiconductor materials thermally connected in parallel and electrically connected in series, where a heat source is applied on one side and part of the thermal flux is converted into electrical energy by means of the Seebeck effect (Figure 1a).

Span et. al. have proposed a new approach to the construction and operation of thermoelectric thin film generators in which a large area PN junction is used not only to mechanically hold the p and n-type semiconductors but to enhance the thermoelectric process by thermal generation and separation of electron hole pairs (EHPs) [7–10].While originally proposed by Span et. al. as a thin film device, it is here transferred to bulk structures. This also removes the difficulties involved with high temperature electrical contacts and the ceramic substrate at the hot side removing the temperature drop across the substrate (Figure 1b).

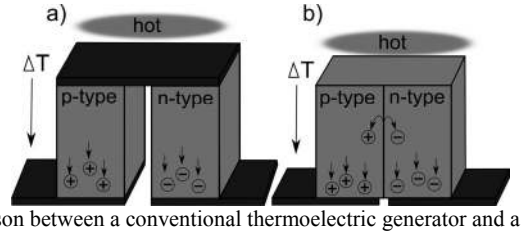

Figure 1. Comparison between a conventional thermoelectric generator and a new concept, originally proposed for thin films TEGs, using large area PN junctions where the contacts at the hot side are not needed.

Although investigation on thermoelectric PN junctions has been reported in [11,12], it was not done in the context proposed by Span et. al. Hence the aim of this paper is to demonstrate that a thermoelectric generator could be built using nanostructured silicon PN junctions which offer the advantage of high temperature operation.

EXPERIMENT

Doped silicon nanoparticles were produced in a bottom up approach starting with a gaseous precursor in a microwave plasma reactor as described in [13]. The doping concentration as calculated from the gas mixture in the plasma reactor is in the order of 10^{20} cm^{-3}. To prepare the PN junctions, a layer of p-type (Boron doped) and a layer of n-type (Phosphorus doped) nanoparticles were densified together in a current assisted sintering process in which Joule heating partially melts the nanoparticles while pressure is applied to the stacked nanoparticles layers thus compacting the nanoparticles into a solid PN junction. Because Peltier effects which are proportional to the electrical current should not be ignored during the compaction process in which kilo-Amperes are forced through the semiconductor material, one PN junction is prepared in ‘forward bias’, and a second sample in ‘reverse bias’ by inverting the stacking order of the nanoparticles powder. Details about the preparation of such PN junctions can be found in [14,15].

The cut densified PN junctions are shown in Figure 2b. The thermoelectric properties are measured in an apparatus schematically depicted in Figure 2a where the temperature gradient is applied parallel to the PN interface with a heating resistor. The cold side is actively cooled with water flowing through the steel sample holder, and mechanical and electrical contacts are made there at the cold side. The temperatures are measured with thermocouples. From this experimental setup, power output, open circuit voltage and short circuit current per temperature difference are characterized.

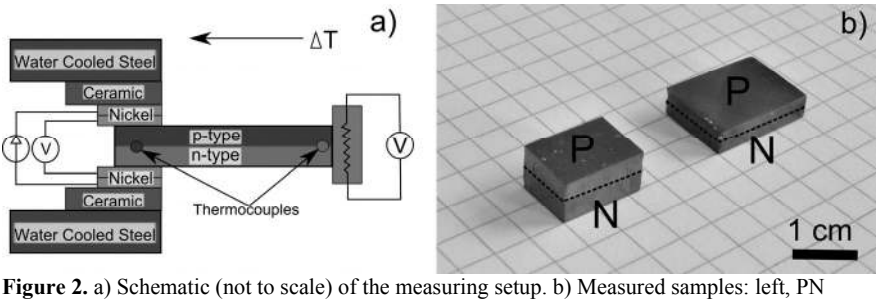

Figure 2. a) Schematic (not to scale) of the measuring setup. b) Measured samples: left, PN Forward, right, PN Reverse. The dotted lines indicate the junction.

RESULTS

First, the electronic properties are summarized. The 4-wire IV characteristics in Figure 3a were obtained at room temperature under thermal equilibrium and dark conditions. Nearly no blocking behavior is observed as opposed to the expectation from a PN junction; this is due to a combination of a number of reasons. For example, during preparation of the PN junction, the n and p-type powders are manually pre-compacted and this creates a great degree of powder intermixing and charge carrier compensation. Moreover, during sintering the partially molten nanoparticles mix further and this can explain why the carrier concentration is lower in the compacted nanoparticles compared to the nominal carrier concentration in the powder [14]. For these reasons, mid bandgap states are formed and this explains the non-blocking behavior of the PN junction in consistency with a Space Charge Limited Current (SCLC) model in which intrinsic shunt paths develop a power dependency of the current from voltage [16]:

$$|I_{SCL}| \propto |V|^{\gamma+1} \quad (2)$$

where $\gamma > 0$ depends on the exact nature of the trap distribution inside the bandgap.

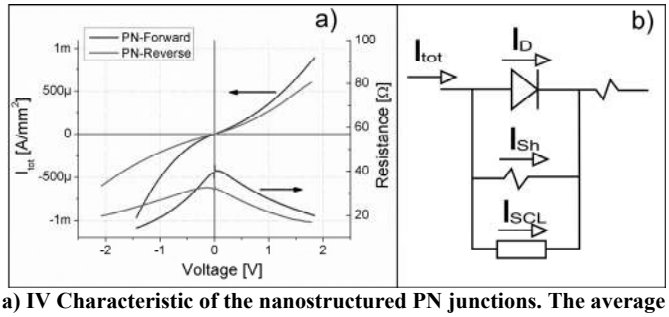

Figure 3 – a) IV Characteristic of the nanostructured PN junctions. The average resistance shows the poor blocking behavior. b) Equivalent circuit of the PN junctions.

Analysis of the equivalent circuit in Figure 3b shows that virtually all the current bypasses the diode, that is $I_{tot} \approx I_{Sh} + I_{SCL}$ as no blocking or exponential behavior is observed.

After subtraction of the linear current I_{Sh} from I_{tot}, the SCLC I_{SCL} can be fitted to a power law fit, from which γ is extracted and follows that $\gamma_{PN\text{-}Forward}=0.46$, $\gamma_{PN\text{-}Reverse}=0.39$, with adjusted R square of .999 for both, showing that the nanostructured PN junctions are best modeled with a linear shunt resistor and a power law SCLC. A small fragment of the PN junction was cut, polished and etched prior to imaging in a scanning electron microscope (SEM). The SEM image in Figure 4 corroborates the poorly defined PN junction and the nanostructure nature of the material which is beneficial for thermoelectric properties.

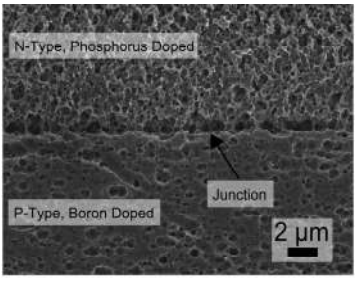

Figure 4 –SEM image shows the poorly defined PN junction and the nanostructured nature of the material.

The thermoelectric properties are investigated using the apparatus in depicted in Figure 2a. The absence of electrical contacts at the hot side allows for temperature gradients larger than 140°C to be applied (the limitation being heating power). Figure 5a shows the IV characteristic from the 'PN Reverse' sample under different temperature gradients. From these IV characteristics the open circuit voltage and short circuit current can be extracted as well as the power generation and internal resistance. Let us first consider the open circuit voltage per temperature difference which closely matches in the samples regardless of preparation (Figure 5b). A coefficient of *Volts/Kelvin* or in other words the equivalent of a Seebeck coefficient is approximated by differentiating the fit of the open circuit voltage in Figure 5b with respect to ΔT. The coefficient of output *Volts/Kelvin* is plotted in Figure 5c and is close compared to the sum of p and n type unipolar coefficients of the same kind of powder earlier reported [17,18].

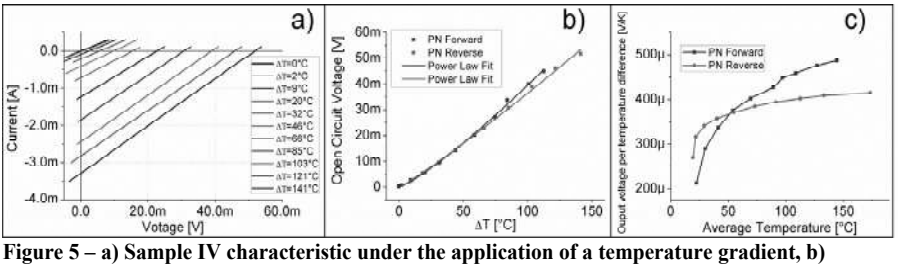

Figure 5 – a) Sample IV characteristic under the application of a temperature gradient, b) device open circuit voltage, c) differentiation of the fits in Figure 5b yields an equivalent output voltage per temperature difference (Seebeck coefficient equivalent).

The total power output and internal resistance can be extracted from Figure 5a, and the maximum power output is plotted in Figure 6a. Because the samples differ in dimension, the power output is normalized by the area and plotted in Figure 6b where it can be seen that regardless of sample preparation, the power generation per unit area matches closely between the two samples. The relatively high internal resistance (Figure 5c) is a considerable limitation in the electrical power output, however, interestingly and opposed to conventional generators, the internal resistance decreases with temperature. This as explained by conventional diode theory, would be due to thermal generation of intrinsic carriers and electron-hole pair separation within the small space charge region domains that might exist because an SCLC model is not expected to be strongly dependent on temperature[16].

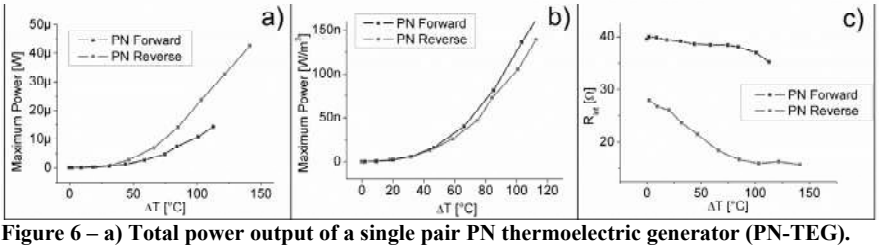

Figure 6 – a) Total power output of a single pair PN thermoelectric generator (PN-TEG). b) Power output normalized by the PN area. c) A decrease of the internal resistance is observed opposite to conventional generators.

Commercial thermoelectric generators or Peltier coolers normally have about 100 pairs for which the concept we propose would produce 4.5mW at $\Delta T \approx 145°C$, this in consideration that ΔT at the present is limited by heating power and not by material stability related issues. The maximum temperature at the hot side is ≈220°C. It is worth noting that in simulations, the PN TEGs are predicted to outperform conventional TEGs for $\Delta T > 300°C$ and that point has not been yet reached [10].

CONCLUSIONS

We demonstrate an alternative concept towards the construction and operation of thermoelectric generators in which a nanostructured PN junction is used to make mechanical and electrical contacts. This makes it possible to apply large temperature gradients > 140°C which are limited by heating power. Power output is characterized along with electronic properties and demonstrates that such an approach is feasible for the construction of high temperature TEGs. Evaluation of the performance of the PN-TEGs and comparison with conventional technologies is due as the main goal here is to demonstrate functionality.

ACKNOWLEDGMENTS

Financial support in the frame of a young investigator grant by the Ministry for innovation, science and research of the State North Rhine Westphalia in Germany is gratefully acknowledged.

REFERENCES

[1] A. Shakouri, Annual Review of Materials Research **41**, 399 (2011).
[2] G.L. Bennett, 26 (2006).
[3] G.L. Bennett and J.J. Lombardo, 26 (2006).
[4] S.K. Bux, R.G. Blair, P.K. Gogna, H. Lee, G. Chen, M.S. Dresselhaus, R.B. Kaner, and J.-P. Fleurial, Advanced Functional Materials **19**, 2445 (2009).
[5] P. Pichanusakorn and P. Bandaru, Materials Science and Engineering: R: Reports **67**, 19 (2010).
[6] C.J. Vineis, A. Shakouri, A. Majumdar, and M.G. Kanatzidis, Advanced Materials (Deerfield Beach, Fla.) **22**, 3970 (2010).
[7] G. Span, M. Wagner, T. Grasser, and L. Holmgren, Physica Status Solidi (RRL) – Rapid Research Letters **1**, 241 (2007).
[8] G. Span, M. Wagner, S. Holzer, and T. Grasser, 2006 25th International Conference on Thermoelectrics 23 (2006).
[9] M. Wagner, G. Span, S. Holzer, and T. Grasser, Semiconductor Science and Technology **22**, S173 (2007).
[10] M. Wagner, G. Span, S. Holzert, and T. Grassert, Simulation 397 (2006).
[11] J.Y. Yang, T. Aizawa, a. Yamamoto, and T. Ohta, Materials Science and Engineering: B **85**, 34 (2001).
[12] P.L. Hagelstein and Y. Kucherov, Applied Physics Letters **81**, 559 (2002).
[13] N. Petermann, N. Stein, G. Schierning, R. Theissmann, B. Stoib, M.S. Brandt, C. Hecht, C. Schulz, and H. Wiggers, Journal of Physics D: Applied Physics **44**, 174034 (2011).
[14] A. Becker, G. Schierning, R. Theissmann, M. Meseth, and N. Benson, Journal of Applied Physics **111**, 054320 (2012).
[15] M. Meseth, P. Ziolkowski, G. Schierning, R. Theissmann, N. Petermann, H. Wiggers, N. Benson, and R. Schmechel, Scripta Materialia **67**, 265 (2012).
[16] S. Dongaonkar, J.D. Servaites, G.M. Ford, S. Loser, J. Moore, R.M. Gelfand, H. Mohseni, H.W. Hillhouse, R. Agrawal, M. a. Ratner, T.J. Marks, M.S. Lundstrom, and M. a. Alam, Journal of Applied Physics **108**, 124509 (2010).
[17] V. Kessler, D. Gautam, T. Hülser, M. Spree, R. Theissmann, M. Winterer, H. Wiggers, G. Schierning, and R. Schmechel, Advanced Engineering Materials n/a (2012).
[18] N. Stein, N. Petermann, R. Theissmann, G. Schierning, R. Schmechel, and H. Wiggers, (2011).

Mater. Res. Soc. Symp. Proc. Vol. 1543 © 2013 Materials Research Society
DOI: 10.1557/opl.2013.938

Thermoelectric transport in topological insulator Bi_2Te_2Se bulk crystals

Yang Xu[1,2], Helin Cao[1,2], Ireneusz Miotkowski[1], Yong P. Chen[1,2]
[1]Department of Physics, Purdue University, West Lafayette, IN 47907 U.S.A
[2]Birck Nanotechnology Center, Purdue University, West Lafayette, IN 47907 U.S.A
[4]School of Electrical and Computer Engineering, Purdue University, West Lafayette, IN 47907 U.S.A

ABSTRACT

Bi_2Te_2Se (BTS221) bulk crystals were recently discovered as an intrinsic 3D topological insulator. We have synthesized this material, and studied the transport properties of BTS221 from the thermoelectrics perspective. Temperature (T) dependent resistivity measurement indicates surface dominant transports in our sample at low T. We also report Seebeck measurement between 50K to room T.

INTRODUCTION

There dimensional (3D) Topological insulator (TI), a new state of quantum matter, has attracted considerable attention mostly because of its unique topological protected surface states (TSS). On the surface of 3D TI materials, there exist non-trivial gapless surface states protected by time-reversal symmetry (TRS), whereas the bulk of TI resembles a normal band insulator. The TSS give rise to 2D helical Dirac fermions with linear energy momentum (E-k) dispersion. Due to the helical nature (resulting in spin-momentum locking) of the Dirac cone(s) on TSS, the topological protection reduces backscattering which requires spin flip (breaking the TRS), and is thus unlikely without magnetic impurities. Therefore, the TSS channels are largely immune to (nonmagnetic) structural imperfection. Because of the characteristic properties, TSS are promising for not only novel physics, but also nano-electronics[1][2][3][4][5]. Among other applications, TI materials are also expected to offer opportunities to enhance energy efficiency of thermoelectric (TE) devices[6][7]. We note that most of the current heavily studied TI materials, such as Bi_2Se_3 and Bi_2Te_3, are also widely-commercialized TE materials with high figure of merit (ZT~1, at ordinary temperatures, ~270 to 400 K). However, both Bi_2Se_3 and Bi_2Te_3 have substantial bulk conduction due to a significant amount of unintentional doping in the bulk. This has been one major challenge for the transport and device studies of TI, as a highly conducting bulk would "short-out" the TSS conduction and mask the transport features associated with TSS.

Recently, a new TI material, Bi_2Te_2Se (BTS221) has been synthesized and demonstrated to have a dominant surface transport at low temperature (T) [8][9]. Here we report our preliminary thermal power (Seebeck coefficient) measurements on bulk BTS221 crystals. Since our BTS221 has been shown to be an intrinsic TI, with bulk insulating and surface conduction dominating at low T [10], studying the Seebeck coefficient of BTS221 at various temperatures (tuning from bulk dominated transport to surface dominated transport as T lowers) will likely provide much insights about thermoelectric transport of TSS and distinguish surface from bulk contributions.

EXPERIMENT

We have synthesized high quality BTS221 crystals by Bridgman method from highly purified (99.9999%) elemental starting materials (Bi, Te and Se). Small pieces of single crystals were cleaved by razor blades, and then fabricated into quasi-Hall bar type devices by attaching contact leads with indium for various transport experiments. In order to perform Seebeck measurements in our cryostat, we built a home-made Seebeck stage. An optical image of the stage is shown in Fig. 1a, and Fig. 1b shows the schematic diagram. On our Seebeck stage, a piece of BTS221 crystal was suspended by two glass substrates. On each substrate, a platinum (Pt) stripe (thickness ~100 nm), serving as a thermometer, was deposited by e-beam evaporation. Temperature dependent four-terminal resistances of each Pt stripe were later measured individually. A pair of thermometers was used to probe temperature gradient ΔT cross the BTS221 crystal by monitoring the resistance change in the Pt stripes. Finally, a film heater was attached to one end of the crystal across which a temperature gradient can be generated by passing electrical current through the heater. After tuning on the heater, we measure voltage difference caused by ΔT, and then calculate S by $\Delta V/\Delta T$. Here we present a representative result measured in a BTS221 crystal (L×W×T ~ 10mm×3mm×200μm).

RESULTS AND DISCUSSION

Figure 1c shows a 4-terminal longitudinal resistance as a function of T from 1.8K to 220K by slowly warming up the sample. The resistivity increases as temperature decreases, indicating an insulating behavior. Our data can be fitted to Arrhenius law ($R_{xx} \sim e^{\Delta/kT}$, where k is the Boltzmann constant, and Δ is an activation energy gap used as the only fitting parameter) very well with Δ ~35meV from 88 K to 220 K as shown in the inset of Fig. 1c. Below 20K, the resistivity begins to saturate. It suggests a surface conduction dominated region. At base temperature, the resistivity reaches ~6 Ω*cm which is comparable to the largest bulk resistivity values have ever been reported in this material[9].

Seebeck coefficient of the BTS221 crystal measured in a mediate T range (between 50 K and 290 K) was shown in Fig. 1d. The positive S indicates a p-type carrier, consistent with the Hall measurement in this sample (data not shown here). As T increases up to room T, S slightly increases. The values of our measured S are found to be comparable to previous measurements [11]. We believe the Seebeck coefficient measured in the mediate T range still involve substantial contribution from the bulk. Interestingly, the value of S at 50 K is notable, and only ~30% lower than that at room T. Future measurements at lower T may be helpful to resolve the surface contribution.

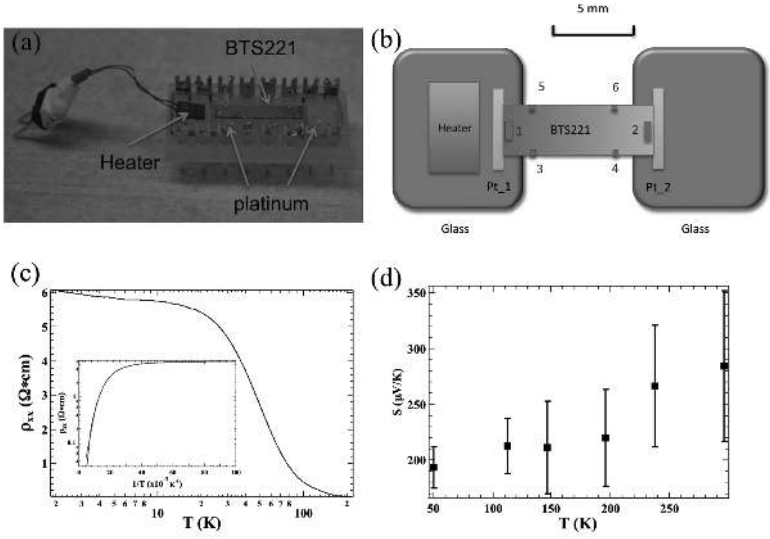

Fig.1. (a) An optical image of one Bi_2Te_2Se single crystal sample mounted on a home-made Seebeck measurement stage. (b) Schematic diagram. (c) Four-terminal R_{xx} (also resistivity) as a function of temperature. An excitation energy ~ 35 meV was extracted by fitting the data to Arrhenius law (as shown in the inset with blue line showing the experimental data and red line the fitting curve). (d) Seebeck coefficient measured in the sample between 50 K and 290 K.

CONCLUSIONS

We have synthesized BT221 crystal. The bulk of the sample is found to be very insulating with a resistivity of ~ 6 Ω*cm at 1.8 K. A home-made Seebeck measurement stage was used to measure the Seebeck coefficient in cryostat. The Seebeck coefficient of our crystal was found to be p-type above 50 K, and can be useful for thermoelectric applications.

ACKNOWLEDGMENTS

We acknowledge support from DARPA MESO program (Grant N66001-11-1-4107).

REFERENCES

[1] J. E. Moore, *Nature* **2010**, *464*, 194–198.

[2] M. Hasan, C. Kane, *Reviews of Modern Physics* **2010**, *82*, 3045–3067.

[3] H. C. Manoharan, *Nature nanotechnology* **2010**, *5*, 477–479.